Acta Crystallographica Section F
Structural Biology and Crystallization Communications
ISSN 1744-3091

Near-atomic resolution analysis of BipD, a component of the type III secretion system of *Burkholderia pseudomallei*

M. Pal,[a,b] P. T. Erskine,[b] R. S. Gill,[b] S. P. Wood[b] and J. B. Cooper[b]*

[a]School of Biological Sciences, University of Southampton, Bassett Crescent East, Southampton SO16 7PX, England, and [b]Laboratory for Protein Crystallography, Centre for Amyloidosis and Acute Phase Proteins, UCL Department of Medicine (Royal Free Campus), Rowland Hill Street, London NW3 2PF, England

Correspondence e-mail: j.b.cooper@medsch.ucl.ac.uk

Received 10 June 2010
Accepted 3 July 2010

PDB Reference: BipD, 3nft.

Burkholderia pseudomallei, the causative agent of melioidosis, possesses a type III protein secretion apparatus that is similar to those found in *Salmonella* and *Shigella*. A major function of these secretion systems is to inject virulence-associated proteins into target cells of the host organism. The *bipD* gene of *B. pseudomallei* encodes a secreted virulence factor that is similar in sequence and is most likely to be functionally analogous to IpaD from *Shigella* and SipD from *Salmonella*. Proteins in this family are thought to act as extracellular chaperones at the tip of the secretion needle to help the hydrophobic translocator proteins enter the target cell membrane, where they form a pore and may also link the translocon pore with the secretion needle. BipD has been crystallized in a monoclinic crystal form that diffracted X-rays to 1.5 Å resolution and the structure was refined to an R factor of 16.1% and an $R_{\rm free}$ of 19.8% at this resolution. The putative dimer interface that was observed in previous crystal structures was retained and a larger surface area was buried in the new crystal form.

1. Introduction

Burkholderia pseudomallei causes the disease melioidosis, which is endemic to tropical and subtropical regions, particularly southeast Asia and northern Australia (Dance, 2002; Gan, 2005). Most commonly, the disease manifests itself clinically as abscesses, pneumonia and, at worst, a fatal septicaemia (Aldhous, 2005; Gan, 2005). The genome of *B. pseudomallei* comprises two chromosomes of 4.07 and 3.17 megabase pairs, which show significant functional partitioning of genes between them (Holden *et al.*, 2004). The large chromosome encodes many of the core functions associated with central metabolism and cell growth, whereas the small chromosome carries more accessory functions associated with adaptation and survival in different environments.

Type III secretion systems (T3SSs) are large assemblies of proteins that span the inner bacterial membrane, the periplasmic space, the peptidoglycan layer, the outer bacterial membrane, the extracellular space and the target cell membrane (Yip & Strynadka, 2006). The function of bacterial protein secretion systems is to transport 'effector' and other proteins across the bacterial inner membrane and the outer envelope in an ATP-dependent manner (Mecsas & Strauss, 1996). Each secretion system involves a hollow tube or needle (the injectisome) through which the secreted proteins travel (Mota *et al.*, 2005). The injectisome varies between 45 and 80 nm in length depending on the bacterial species, is made by the polymerization of a major subunit and has a hollow interior of approximately 25 Å in diameter. The ring-like assembly that spans the membrane of the host cell is referred to as the translocon. This is formed by the initial secretion of a small number of proteins into the extracellular environment as a result of contact between the bacterium and the target cell (Pettersson *et al.*, 1996). The translocator proteins act to transport bacterial proteins across the plasma membrane into the host cell, where they essentially subvert the cell's normal processes to aid replication of the bacterium. It appears that the translocator proteins

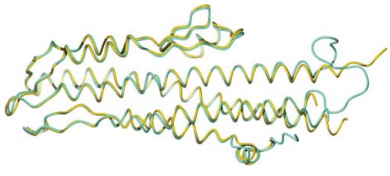

Table 1
Data-collection and refinement statistics for BipD.

Values in parentheses are for the outer resolution shell.

Data processing	
Space group	*C*2
Unit-cell parameters	
a (Å)	51.15
b (Å)	60.42
c (Å)	90.42
β (°)	96.01
Resolution range (Å)	38.9–1.5 (1.6–1.5)
$R_{\rm merge}$† (%)	6.7 (55.6)
No. of reflections	218736 (21656)
No. of unique reflections	42898 (6210)
Mean $I/\sigma(I)$	13.7 (2.0)
Completeness (%)	98.3 (99.4)
Multiplicity	5.1 (3.5)
Refinement	
No. of atoms in protein	2089
No. of solvent atoms	259
Resolution range (Å)	34.7–1.5
No. of reflections in working set	40761
No. of reflections in free set	2038
R factor (%)	16.1
$R_{\rm free}$ (%)	19.8
R.m.s. bond-length deviation (Å)	0.012
R.m.s. bond-angle deviation (°)	1.26

† $R_{\rm merge} = 100 \times \sum_{hkl} \sum_i |I_i(hkl) - \langle I(hkl)\rangle| / \sum_{hkl} \sum_i I_i(hkl)$, where $\langle I(hkl)\rangle$ is the mean intensity of the scaled observations $I_i(hkl)$.

form a pore in the lipid membrane of the target cell through which the effector proteins are able to pass (Blocker *et al.*, 2000). Interestingly, the T3SS and the flagellar motor have several common protein components, which together with the ability of flagella to secrete certain proteins suggests a common evolutionary origin (Yip & Strynadka, 2006).

It has been found that *B. pseudomallei* contains at least three loci encoding putative type III protein secretion systems (Rainbow *et al.*, 2002), one of which shares homology with one of the T3SSs of *Salmonella typhimurium* (Attree & Attree, 2001) and *Shigella flexneri* (Stevens *et al.*, 2002) and has been designated as the *Burkholderia* secretion apparatus or BSA (Hueck, 1998). The BSA effector proteins are termed Bop proteins and the translocators are termed Bip proteins (short for *Burkholderia* invasion proteins). In *Salmonella* the homologous proteins SipB, SipC and SipD are required for the injection of effector molecules and the invasion of epithelial cells *in vitro* (Kaniga *et al.*, 1995) and likewise for IpaB, IpaC and IpaD from *Shigella* (Ménard *et al.*, 1994). Hence, it is thought that the *B. pseudomallei* homologues BipB, BipC and BipD perform a similar function. Disruption of the *bipD* gene reduces the ability of *B. pseudomallei* to invade eukaryotic cells and reduces virulence in mice (Stevens *et al.*, 2002, 2004), indicating that the BipD protein is an important secreted virulence factor. A BipD mutant exhibited impaired invasion of HeLa cells, reduced intracellular survival in murine macrophage-like cells and a marked reduction in actin-tail formation (Stevens *et al.*, 2002, 2004). Hence, it has been suggested that BipD is involved in the actin polymerization that facilitates the escape of *B. pseudomallei* from endocytic vesicles during the initial infection and the subsequent escape of progeny bacteria into surrounding host cells. It has also been suggested that proteins in the same class as BipD (*e.g.* IpaD and SipD) act as extracellular chaperones to help the hydrophobic translocators (equivalent to BipB and BipC) enter the target cell membrane and may even link the translocon pore with the secretion needle (Mecsas & Strauss, 1996).

The BipD protein from *B. pseudomallei* consists of 310 amino acids and has a molecular weight of 33 kDa. Recently, the biophysical properties of BipD and its homologues have been extensively analysed by Espina *et al.* (2007) and their role in the type III secretion system has been reviewed in Moraes *et al.* (2008). Previously, we have crystallized BipD in a monoclinic crystal form that diffracted X-rays to 2.1 Å resolution and determined its structure by selenomethionine MAD (Knight *et al.*, 2006; Erskine *et al.*, 2006) in parallel with similar studies elsewhere (Roversi *et al.*, 2006; Johnson *et al.*, 2007). In this paper, we report that the crystallization of the BipD protein in the presence of the lipid head-group phosphocholine gave a crystal form that diffracted to 1.5 Å resolution, thus allowing the structure to be refined at near-atomic resolution.

2. Crystallization of BipD

The expression of BipD in *Escherichia coli* as a GST-fusion protein and affinity purification have been described elsewhere (Knight *et al.*, 2006) together with the crystallization of the native protein. In the current study, the expressed BipD protein was concentrated to 6 mg ml^{-1} (as determined using a Nanodrop ND1000 spectrophotometer at 280 nm) in 10 m*M* Tris–HCl, 140 m*M* NaCl pH 7.5. Crystals were obtained by inclusion of phosphocholine in the mother liquor since preliminary isothermal titration calorimetric studies had suggested that this compound interacted with the protein, although the result was difficult to reproduce. Use of Molecular Dimensions Structure Screens I and II and subsequent optimization of hits established that the best crystals could be obtained in 35%(*w*/*v*) PEG 4000, 100 m*M* glycine, 20 m*M* EDTA, 60 m*M* cacodylate buffer pH 6.0. Using the hanging-drop method, 2 µl protein solution was mixed with 2 µl 10 m*M* phosphocholine (in 10 m*M* Tris–HCl pH 7.5) and 4 µl well solution on siliconized glass cover slips. The crystals, which appeared in 2–3 weeks (Fig. 1), were cryoprotected with 30% glycerol (added stepwise) and mounted in loops for flash-freezing with an Oxford Cryosystems cryostat and subsequent storage under liquid nitrogen.

3. X-ray data collection and processing

Data were collected at Diamond Light Source (UK) on beamline I02 (λ = 0.976 Å) with an ADSC Q315 CCD detector and with the sample maintained at a temperature of 100 K. The crystal diffracted to a resolution of at least 1.5 Å and 360 images were collected with an oscillation angle of 0.5°. The data were processed in space group *C*2 using *iMOSFLM* (Leslie, 2006), *SCALA* (Evans, 2006), *TRUNCATE* (French & Wilson, 1978) and other utilities in the *CCP*4 program suite (Collaborative Computational Project, Number 4, 1994). The corresponding unit-cell parameters were a = 51.15, b = 60.42, c = 90.42 Å, β = 96.01°. The Matthews coefficient (Kantardjieff &

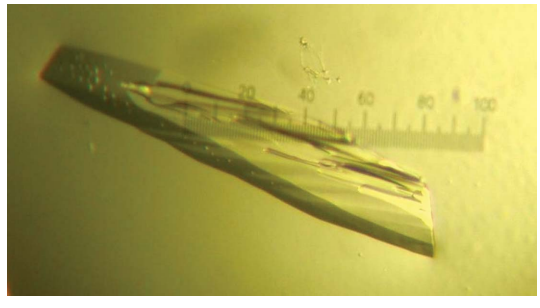

Figure 1
The crystal of BipD which diffracted to beyond 1.5 Å resolution. The crystal is approximately 1.0 mm in its largest dimension.

Rupp, 2003; Matthews, 1968) was calculated using the program *MATTHEWS_COEF* (Collaborative Computational Project, Number 4, 1994), which suggested the presence of only one BipD molecule in the asymmetric unit, with a solvent content of 42%. The data set had overall and outer shell $R_{\rm merge}$ values of 6.7% and 55.6%, respectively (Table 1).

4. Structure determination

One monomer of the previously solved structure of BipD (Erskine *et al.*, 2006; PDB code 2izp) was used as the search model in molecular replacement using *Phaser* (Read, 2001). Of the possible alternative space groups, only one (*C*2) yielded a solution (rotational *Z* score 16.7, translational *Z* score 13.6, log-likelihood gain 1788) which gave good crystal packing. The model was then subjected to several rounds of refinement with *REFMAC* (Murshudov *et al.*, 1997) and rebuilding using *Coot* (Emsley & Cowtan, 2004) and 259 water molecules were added. After anisotropic temperature-factor refinement, the final *R* factor and $R_{\rm free}$ were 16.1% and 19.8%, respectively (Table 1). The coordinates and structure factors have been deposited in the Protein Data Bank (http://www.wwpdb.org) with accession code 3nft. The significance of putative oligomeric states arising from symmetry operations of the new crystal form were analysed by use of the *PISA* server provided by the European Bioinformatics Institute (Krissinel & Henrick, 2007).

Continuous electron density was visible for most of the protein except for the first 33 N-terminal residues, the loop formed by residues 113–121 and six residues at the C-terminal end. A sample of the electron density showing its appreciable atomicity is shown in Fig. 2. The current structure superimposes on the previous structure with an r.m.s. deviation of 0.65 Å for the 253 equivalent C^{α} atoms that are closer than 3.5 Å following least-squares fitting (Fig. 3). Residues 104–112, which were rather poorly defined in the previous electron-density map at 2.1 Å resolution (Erskine *et al.*, 2006), are extremely well defined in the new map, thus improving the definition of the final 2–3 turns of helix α3. The same improvement in map quality is seen for residues at the other end of this loop in the range 125–128 which lead into helix α4 and are involved in putative dimer interactions.

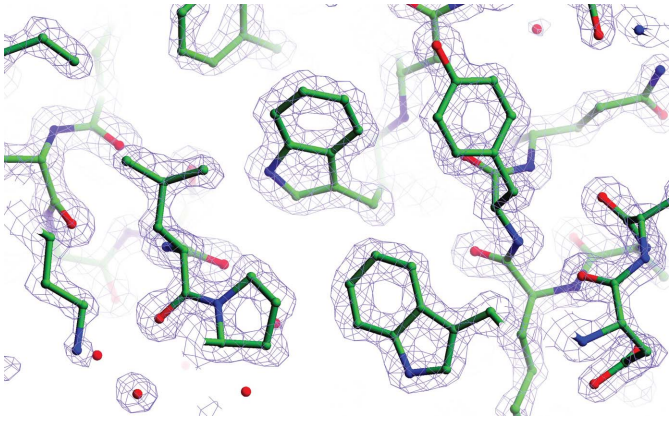

Figure 2
A sample of the $2F_{\rm o} - F_{\rm c}$ electron-density map at 1.5 Å resolution contoured at 2 r.m.s. (blue contours).

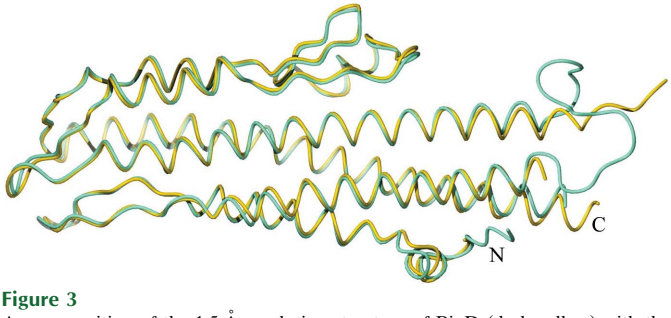

Figure 3
A superposition of the 1.5 Å resolution structure of BipD (dark yellow) with the previous model solved at 2.1 Å resolution (cyan) in a different space group. The only regions where the structures differ appreciably were very poorly defined in the earlier analysis.

Interestingly, the putative dimer interface relating the two monomers in the asymmetric unit of the earlier crystal form (shown in Fig. 7 of Erskine *et al.*, 2006) is conserved in the new crystal form, with the only differences being that in the new form the two monomers are re-oriented slightly and are related by crystallographic rather than noncrystallographic symmetry. These interactions involve helices α4 and α8 pairing with their counterparts in the adjacent monomer in an antiparallel manner owing to an intervening (pseudo)twofold axis. The C-terminal end of α8 is the most highly conserved region of the molecule. The total surface-accessible area of each monomer that is buried in this putative dimer interface (1271 Å^2) is larger than that reported for the previous crystal form (970 Å^2; Erskine *et al.*, 2006). The apparent strengthening of the dimer interface may stem from the improved definition of the residues in the range 125–128 which form more extensive contacts in the new crystal form. It is interesting that the same putative dimer interface is observed in yet further crystal forms of BipD that have been reported by others (Johnson *et al.*, 2007; PDB codes 2ixr and 2j9t). Intriguingly, the putative ligand (phosphocholine) was not visible in the electron-density map, although it appears to have acted as a crystallization additive in producing the significantly improved crystal form which we report here.

We thank the Gerald Kerkut Charitable Trust for a studentship to MP. We are indebted to Diamond Light Source for beam time and travel support.

References

Aldhous, P. (2005). *Nature (London)*, **434**, 692–693.
Attree, O. & Attree, I. (2001). *Microbiology*, **147**, 3197–3199.
Blocker, A., Holden, D. & Cornelis, G. (2000). *Cell. Microbiol.* **2**, 387–390.
Collaborative Computational Project, Number 4 (1994). *Acta Cryst.* D**50**, 760–763.
Dance, D. A. (2002). *Curr. Opin. Infect. Dis.* **15**, 127–132.
Emsley, P. & Cowtan, K. (2004). *Acta Cryst.* D**60**, 2126–2132.
Erskine, P. T., Knight, M. J., Ruaux, A., Mikolajek, H., Wong Fat Sang, N., Withers, J., Gill, R., Wood, S. P., Wood, M., Fox, G. C. & Cooper, J. B. (2006). *J. Mol. Biol.* **363**, 125–136.
Espina, M., Ausar, S. F., Middaugh, C. R., Baxter, M. A., Picking, W. D. & Picking, W. L. (2007). *Protein Sci.* **16**, 704–714.
Evans, P. (2006). *Acta Cryst.* D**62**, 72–82.
French, S. & Wilson, K. (1978). *Acta Cryst.* A**34**, 517–525.
Gan, Y.-H. (2005). *J. Infect. Dis.* **192**, 1845–1850.
Holden, M. T. G. *et al.* (2004). *Proc. Natl Acad. Sci. USA*, **101**, 14240–14245.
Hueck, C. J. (1998). *Microbiol. Mol. Biol. Rev.* **62**, 379–433.
Johnson, S., Roversi, P., Espina, M., Olive, A., Deane, J. E., Birket, S., Field, T., Picking, W. D., Blocker, A. J., Galyov, E. E., Picking, W. L. & Lea, S. M. (2007). *J. Biol. Chem.* **282**, 4035–4044.
Kaniga, K., Trollinger, D. & Galan, J. E. (1995). *J. Bacteriol.* **177**, 7078–7085.
Kantardjieff, K. A. & Rupp, B. (2003). *Protein Sci.* **12**, 1865–1871.
Knight, M. J., Ruaux, A., Mikolajek, H., Erskine, P. T., Gill, R., Wood, S. P., Wood, M. & Cooper, J. B. (2006). *Acta Cryst.* F**62**, 761–764.
Krissinel, E. & Henrick, K. (2007). *J. Mol. Biol.* **372**, 774–797.
Leslie, A. G. W. (2006). *Acta Cryst.* D**62**, 48–57.
Matthews, B. W. (1968). *J. Mol. Biol.* **33**, 491–497.
Mecsas, J. & Strauss, E. J. (1996). *Emerg. Infect. Dis.* **2**, 271–288.

Ménard, R., Sansonetti, P. & Parsot, C. (1994). *EMBO J.* **13**, 5293–5302.
Mota, L. J., Sorg, I. & Cornelis, G. R. (2005). *FEMS Microbiol. Lett.* **252**, 1–10.
Moraes, T. F., Spreter, T. & Strynadka, N. C. J. (2008). *Curr. Opin. Struct. Biol.* **18**, 258–266.
Murshudov, G. N., Vagin, A. A. & Dodson, E. J. (1997). *Acta Cryst.* D**53**, 240–255.
Pettersson, J., Nordfelth, R., Dubinina, E., Bergman, T., Gustafsson, M., Magnusson, K. E. & Wolf-Watz, H. (1996). *Science*, **273**, 1231–1233.
Rainbow, L., Hart, C. A. & Winstanley, C. (2002). *J. Med. Microbiol.* **51**, 374–384.
Read, R. J. (2001). *Acta Cryst.* D**57**, 1373–1382.
Roversi, P., Johnson, S., Field, T., Deane, J. E., Galyov, E. E. & Lea, S. M. (2006). *Acta Cryst.* F**62**, 861–864.
Stevens, M. P., Haque, A., Atkins, T., Hill, J., Wood, M. W., Easton, A., Nelson, M., Underwood-Fowler, C., Titball, R. W., Bancroft, G. J. & Galyov, E. E. (2004). *Microbiology*, **150**, 2669–2676.
Stevens, M. P., Wood, M. W., Taylor, L. A., Monaghan, P., Hawes, P., Jones, P. W., Wallis, T. S. & Galyov, E. E. (2002). *Mol. Microbiol.* **46**, 649–659.
Yip, C. K. & Strynadka, N. C. J. (2006). *Trends Biochem. Sci.* **31**, 223–230.